



Residual Performance of Structural Steel Beams after Plastic Deformation and Strain Aging

K. Taniguchi ⁽¹⁾, S. Yang ⁽²⁾, T. Okazaki ⁽³⁾, T. Asari ⁽⁴⁾

⁽¹⁾ Graduate student, Graduate School of Engineering, Hokkaido University, kayo-taniguchi@eis.hokudai.ac.jp

⁽²⁾ Ph.D. student, Department of Civil Engineering and Applied Mechanics, McGill University, Shaoqi.yang@mail.mcgill.ca

⁽³⁾ Professor, Faculty of Engineering, Hokkaido University, tokazaki@eng.hokudai.ac.jp

⁽⁴⁾ Assistant Professor, Faculty of Engineering, Hokkaido University, asari@eng.hokudai.ac.jp

Abstract

Steel is very well suited for sustainable construction owing to its recyclable and durable properties. Today, nearly all structural steel is reused after the service life of the building is ended. However, because the recycle process (from steel scrap to new steel) requires abundant energy consumption and associated carbon-dioxide emission, the sustainability of steel construction can be further promoted by establishing reuse: procuring steel components from a building during the demolition stage, refurbish and then reusing those components in a new structure. To do so, the performance of used steel must be evaluated. Any change in structural properties from newly produced steel caused by fabrication, transportation, construction, service, and extraction, needs to be quantified. Most significantly, the effect of plastic deformation due to earthquake loading, large or small, and subsequent strain aging needs to be quantified.

Therefore, research was conducted to understand the residual performance of common Japanese rolled I-sections, all produced by the blast furnace process, after plastic deformation and strain aging. The research program comprised three experiments: (1) monotonic tension coupon tests, (2) cyclic tension-and-compression coupon tests and (3) cyclic-loading beam tests. The tests were conducted in two phases: first, monotonic or cyclic loading was conducted to predetermined plastic deformation, and subsequently, after curing at ambient temperature for 30 or 90 days, loading was resumed until specimen failure. The beam tests were halted at cyclic amplitudes of 0.01 or 0.02 rad where the elastic limit was slightly greater than 0.005 rad. To provide a point of comparison, each specimen set included one specimen tested in a single phase with no intermediate curing.

As expected from findings reported in the literature, the change in tensile properties was influenced by the extent of pre-strain and free nitrogen content. Larger pre-strain caused greater change in mechanical properties. Among three steel samples, SS400 with free nitrogen content of 0.006% saw the most profound change in tension properties, while SN400B and SN490B with free nitrogen content of 0.003 and 0.002%, respectively, saw very little change. During the first half cycle after 0.01 or 0.02-rad pre-strain and curing, SS400 beams exhibited a yield plateau that was not seen in the specimen with no pre-strain. The significantly higher plateau strength diminished within one or two positive-and-negative loading cycles. The strain aging produced by 0.01 or 0.02-rad pre-strain did not affect the cyclic loading response of the SS400 beams at ± 0.04 rad. In other words, the plastic deformation capacity of the beam was not affected by strain aging. Further tests will be conducted to establish the correlation between steel grade, free nitrogen content and plastic loading history on the residual performance or structural steel.

Keywords: Steel structures, Residual performance, Strain aging, Plastic deformation, Cyclic-loading tests

1. Introduction

Steel is very well suited for sustainable construction owing to its recyclable and durable properties. Today, nearly all structural steel is reused after the service life of the building is ended. However, because the recycle process (from steel scrap to new steel) requires abundant energy consumption and associated carbon-dioxide emission, the sustainability of steel construction can be further promoted by establishing reuse: procuring steel components from a building during the demolition stage, refurbish and then reusing those components in a new structure. In order to establish reuse of steel components, the residual performance of used steel must be evaluated. Any change in structural properties from newly produced steel caused by fabrication, transportation, construction, service, and extraction, needs to be quantified. In most cases, the reusability of used steel may be easily judged based on visual inspection of chemical or physical changes. For example, unless exposed to corrosive environments, which is limited to special use, structural steel in buildings does not degrade during service due to chemical causes. Segments severely altered by welding, trimming, protrusions, cambering, etc., may be unsuitable for reuse. However, scientific basis is needed to judge the reusability of steel affected by earthquake loading, large or small, especially in a seismically active environment like Japan where a large proportion of buildings experience earthquakes during their service life. To be specific, severe earthquakes can cause plastic deformation in steel components, and during subsequent service of the building, the properties of these steel components can change due to strain aging, a phenomenon observed in many types of metal. Therefore, towards the larger goal of promoting steel reuse, an experimental program is conducted to quantify the effect of plastic deformation and subsequent strain aging on the residual structural performance of structural steel components.

“Strain aging” is a phenomenon observed in steel which, as illustrated in Fig. 1, causes increased yield strength, recovery of a sharp yield point, and reduced ductility and toughness [1, 2]. Strain aging is significantly affected by chemical composition of the steel and curing environment. Cottrell and Bilby [3] explained that strain aging of low carbon steel is caused by segregation of interstitial carbon and nitrogen atoms to form atmospheres around dislocations. Based on a review of over 30 types of steel, Pense [4] stated that strain aging can occur in any steel. Inelastic strain introduced at ambient temperature causes strain aging, but the effect may be relaxed depending on the temperature maintained over the duration when strain aging takes effect: temperature up to 426°C has no relaxing effect; temperatures between 482 and 649°C can relax ductility loss; temperature above 649°C can relax the change in yield and tensile strength and elongation but not to the original properties.

Wilson and Russell [5] reported for low-carbon rimmed steel that changes in yield strength and elongation is controlled by grain size and content of dissolved carbon and nitrogen and that the effect saturates after 1 week at 60°C. Succop et al. [6] observed for pressure-vessel steel that even a small, 1.25% pre-strain can cause 75% increase in yield strength after 3,000 hours at 260°C. They suggested that 260 to 343°C might be the most detrimental curing temperature. Kaufmann et al. [7] studied strain aging in the

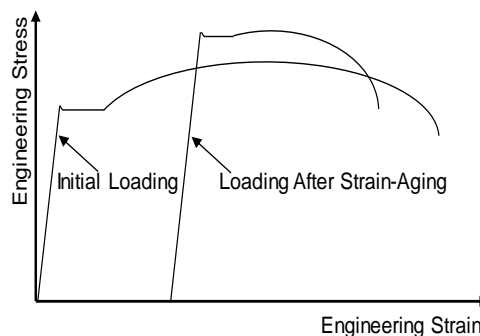


Fig. 1 – Strain-aging effect seen in tension coupon tests

context of k-area properties of rolled I-sections. Three steels produced at different time were compared to address the change in milling process from blast furnace to electric arc furnace in the US in 1980's. In the range of 2 to 12%, larger pre-strain caused larger increase in yield strength, from 20 to 40%. In steel cured after 12% pre-strain, which stressed the material to near the necking point, the yield plateau re-appeared but strain hardening was negligible. Mojtaba [8] observed for SN490B steel that increase in yield strength was independent of the amount of pre-strain and that strain hardening rate did not change with aging. In Japan, Ono et al. [9] observed for SN490 steel, out of interest in the seismic performance of cold-formed hollow-structural shapes, that strain aging is prominent in steel with free nitrogen content greater than 0.003%. Yamada et al. [10] observed for SS400 steel that strain aging may saturate at 3 months under ambient temperature. They also observed from cyclic-loading tests of beam-to-column connections made of SS400 steel that strain aging can result in a favorable distribution of tension properties to promote yielding in regions away from critical welds.

2. Experimental Program

Hot-rolled H-500×200×10×16 sections of three different structural steel grades, Japanese Industry Standard (JIS) SS400, SN400B and SN490B, all produced by the blast furnace process, were selected for the study. These are among the most common and widely used steel grades in Japan: SS400 (minimum specified yield strength, $\sigma_y \geq 235$ N/mm²) is an older grade whose origin dates back to 1952; SN400B ($\sigma_y \geq 235$ N/mm²) and SN490B ($\sigma_y \geq 325$ N/mm²) are currently the most common grade for the primary load bearing system. Table 1 lists the mechanical properties and key chemical composition. The mechanical properties were established from the tension coupon tests described later. Carbon content was taken from mill test reports. The total and free nitrogen content was measured according to JIS G 1228: *Iron and steel – Methods for determination of nitrogen content*. Total nitrogen was measured based the thermal conductimetric method while nitrogen contained as nitride was measured based on the spectrophotometric method. Free nitrogen was computed as total nitrogen less nitrogen as nitride. For all three samples, free nitrogen content was nearly identical to total nitrogen content. Between the three grades, SS400 had notably larger total and free nitrogen content than SN400B or SN490B.

The three steel samples were used to conduct three different experiments: (1) monotonic tension coupon tests, (2) cyclic tension-and-compression coupon tests and (3) cyclic-loading beam tests. At the time of this writing, (1) is completed, (2) is underway, and (3) is partly completed.

For experiment (1), JIS 1A tension coupons were extracted from the flange or web of the I-sections. An extensometer was devised to measure engineering strain over the standard gauge length of 200 mm. The coupons were pre-strained to three different values, 2, 4 and 8%, and then cured at room temperature for 1 or 3 months. After the designated curing period, the pre-strained coupons were tested to fracture. A fourth coupon was tensioned to fracture with no pre-strain to provide data on properties without strain aging. The tests were conducted using a 1,000-kN capacity universal testing machine. The strain rate was controlled at 0.00005 /s until the start of strain hardening, 0.00025 /s until the tensile strength was measured, and then

Table 1 – Mechanical and chemical properties

Grade	SS400		SN400B		SN490B	
	Flange	Web	Flange	Web	Flange	Web
Yield strength [N/mm ²]	300	332	284	322	344	358
Tensile strength [N/mm ²]	448	462	457	472	521	522
Elongation [%]	31	28	33	29	29	25
Yield-to-tensile ratio	0.67	0.72	0.62	0.68	0.66	0.69
Carbon content [wt%]	0.15		0.16		0.16	
Total nitrogen content [wt%]	0.0073		0.0031		0.0028	
Free nitrogen content [wt%]	0.006		0.003		0.002	

0.0005 /s to fracture.

Experiment (2), which is underway, uses JIS 1A tension coupons extracted from the flanges only. Two coupons will be loaded according to a cyclic loading protocol to a strain amplitude of ± 0.01 or $\pm 0.02\%$. The coupons will be unloaded to zero strain, and then cured at room temperature for 3 months or longer, before resuming the cyclic loading protocol. A third specimen will be loaded with no pre-strain to provide data on performance without strain aging. Results from Experiment (2) are not reported in this paper.

Fig. 2 shows the test setup for Experiment (3). The specimen comprises a beam stub welded to an end plate. The beam and loading beam are laterally braced to limit lateral-torsional deformation. As cyclic load is applied to the beam, the beam stub experiences inelasticity while all components outside of the specimen remain elastic and undamaged. The beam stub is welded to the end plate using the no-weld-access hole beam-to-column moment-connection detail that is commonly adopted in Japan today. Loading was controlled according to the US cyclic loading program for prequalification testing of moment-frame connections: The cyclic story-drift angle was gradually increased from ± 0.002 , ± 0.00375 , ± 0.005 , ± 0.0075 , ± 0.01 , ± 0.015 , ± 0.02 , ± 0.03 , to ± 0.04 rad. Three cycles were repeated for each angle up to ± 0.01 rad, and afterwards two cycles were repeated for each angle. Three specimens for SS400 steel have been completed. Two of the specimens were first loaded to a cyclic angle of ± 0.01 or ± 0.02 rad, unloaded to zero story drift, and then cured at room temperature for 3 months before resuming the cyclic loading program. A third specimen was loaded with no pre-strain to provide data on performance without strain aging.

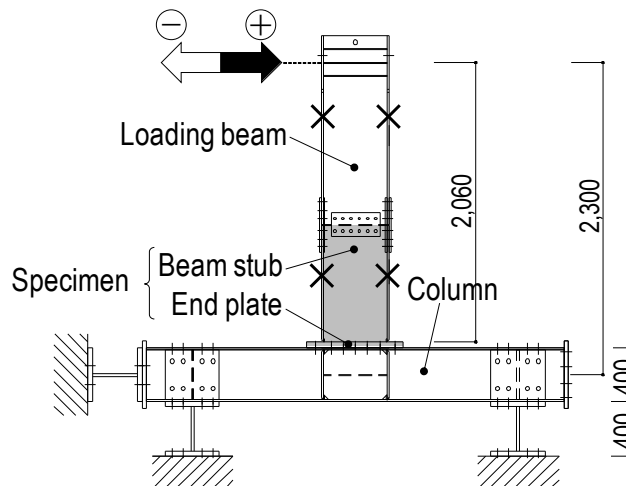


Fig. 2 – Test setup for cyclic-loading beam tests

3. Results from Monotonic Coupon Tests

Fig. 3 shows some of the strain-stress relationships obtained from the flanges. The mechanical properties listed in Table 1 including yield strength was established from the coupon indicated in the figures as 0% pre-strain. Change in tension properties caused by strain aging was noticed as re-appearance of distinguishable yield plateau, rise in yield strength, rise in tensile strength, and reduction in elongation with respect to the original properties. No significant difference was observed between the curing periods of 1 or 3 months (Note: figure shows the two curing cases only for SS400 steel). For all three grades, larger pre-strain resulted in larger change in tension properties: 8% pre-strain resulted in recovery of upper-yield point and yield plateau, with 40 to 60% strength increase at the plateau. Little change in tensile strength was observed: 8% pre-strain resulted in 4% increase in SS400 but no significant change in SN400B and SN490B. Little change in elongation was observed: 8% pre-strain resulted in 15% reduction in SS400 but no significant change in SN400B and SN490B. Consequently, among the three grades of steel, SS400 saw the most profound changes in tensile properties, while SN400B and SN490B saw very little change. The result correlated with the

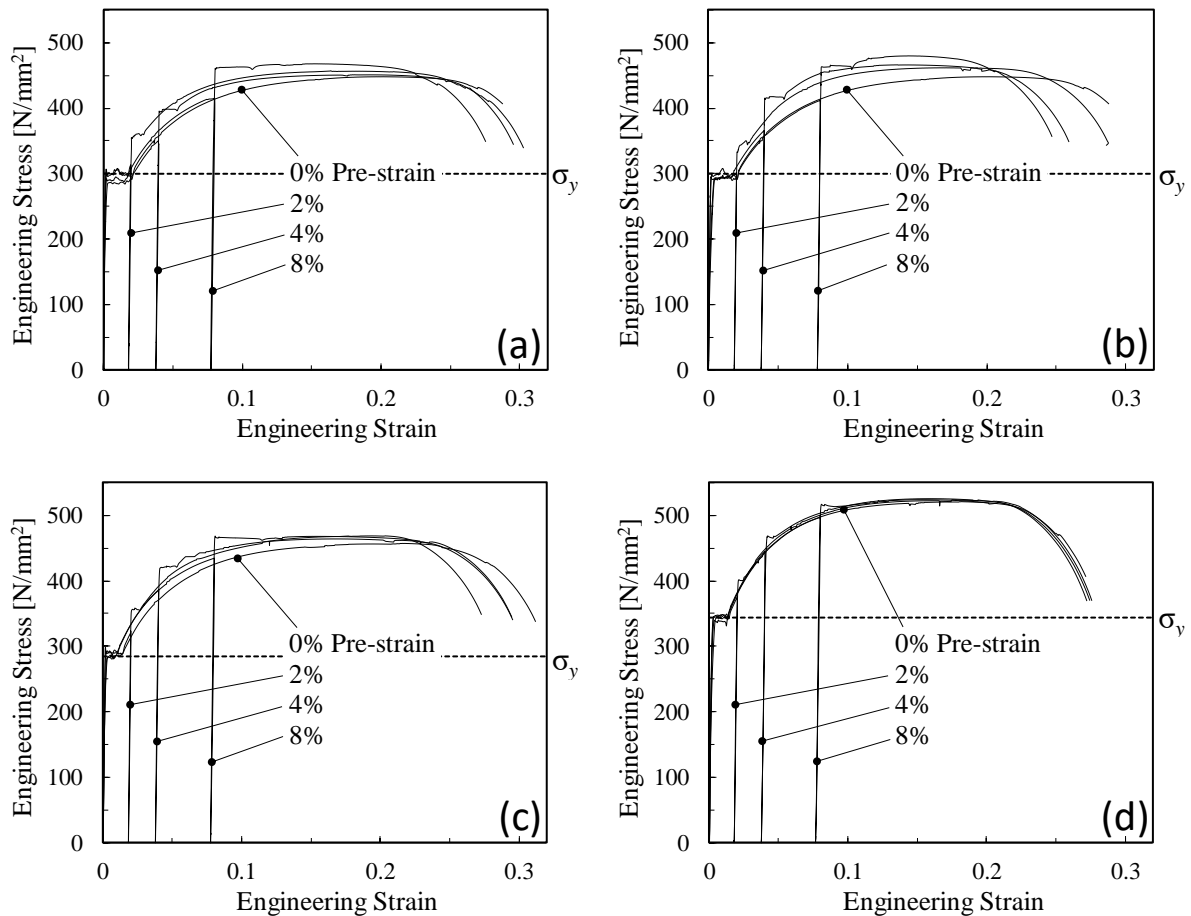


Fig. 3 – Stress-strain relationships obtained from two-stage coupon tension tests: (a) SS400 steel with 1-month curing; (b) SS400 steel with 3-month curing; (c) SN400B steel with 3-month curing; (d) SN490B steel with 3-month curing.

nitrogen content listed in Table 1: the free nitrogen content was 0.006% for SS400 but 0.003 and 0.002%, respectively, for SN400B or SN490B.

The change in yield strength and elongation for SS400 steel was consistent with the report by Yamada et al. [10] The rise in tensile strength was notably smaller than the results reported by Yamada et al. [10] and Pense [4]. Based on these observations, it was deemed that the curing period of three months is enough to obtain the full effect of strain aging from the three samples of steel.

4. Results from Cyclic-Loading Beam Tests

Fig. 4 shows the cyclic-loading hysteresis obtained from three specimens of SS400 steel, plotting the beam-end moment against story-drift angle. The pre-strain stage of loading is indicated by dotted lines while the loading after 3-month curing is indicated by solid lines. The plastic moment, M_p , based on the original yield strength, listed in Table 1, is shown as reference. All three specimens responded elastically at ± 0.005 rad, but started to yield during ± 0.0075 rad. When the loading protocol was completed with two cycles at ± 0.04 rad, the strength of the specimen had dropped to 85% of the maximum recorded value. The primary cause of strength degradation was local flange and web distortion. Local flange distortion formed during ± 0.02 rad, strength degradation started during ± 0.03 rad, and substantial flange and web distortion had formed by the end of the test. Cracks formed between the complete-joint-penetration groove weld and beam flange during ± 0.02 rad but these cracks had not developed significantly at the end of the test.

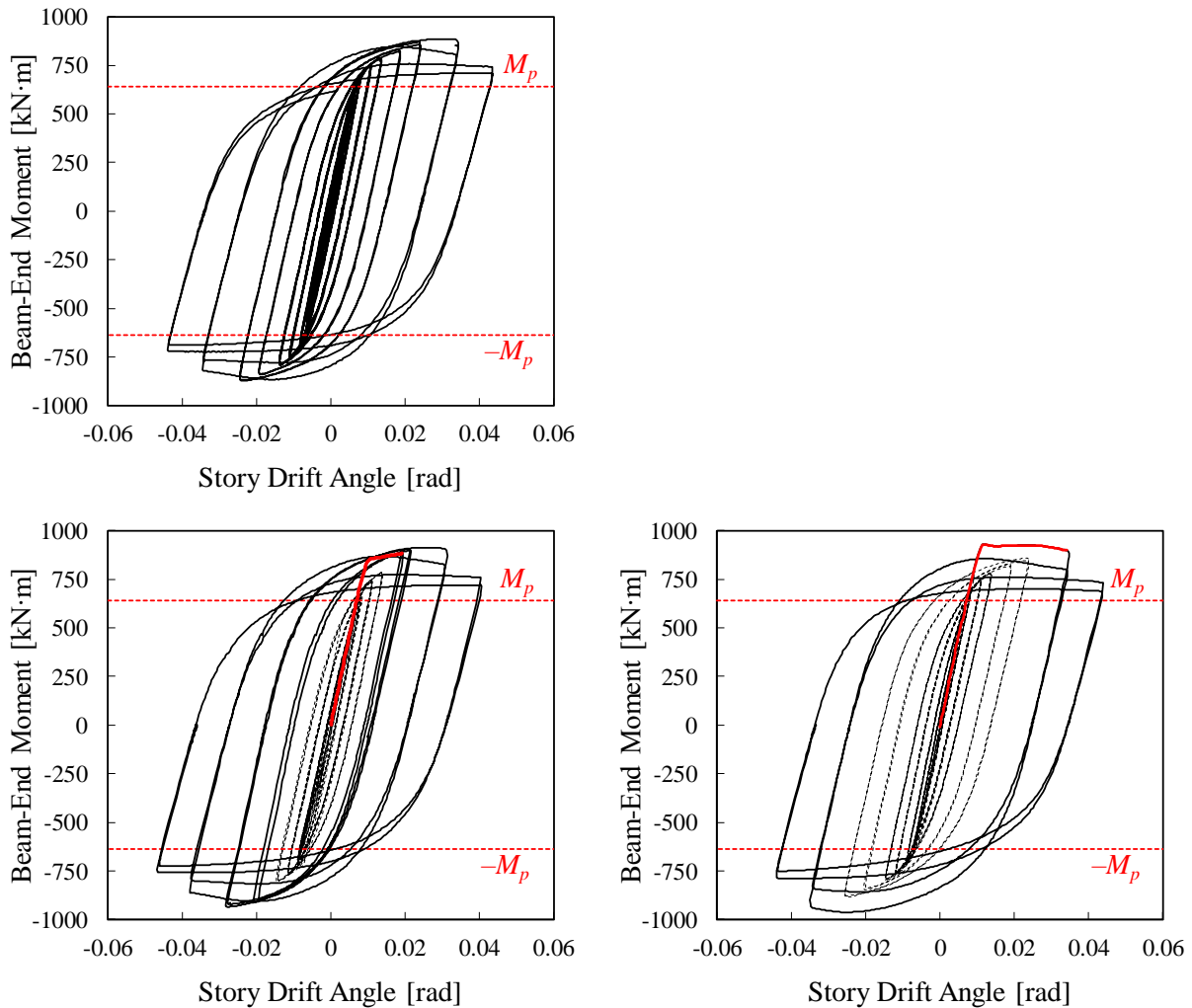


Fig. 4 – Loading curves obtained from cyclic-loading tests of SS400 beams: (a) no pre-strain; (b) with 0.01-rad pre-strain; (c) with 0.02-rad pre-strain.

Although not present in the specimen with no pre-strain, the specimens with 0.01 or 0.02-rad pre-strain exhibited a yield plateau during the first half cycle after curing. The strength at the plateau was 1.32 and 1.43 times M_p , respectively, for the specimens with 0.01 and 0.02-rad pre-strain. However, the difference in response between the specimen with and without pre-strain diminished within one or two positive-and-negative loading cycles. To be specific, the specimen with 0.01-rad pre-strain exhibited larger strength than the specimen with no pre-strain during the ± 0.015 rad cycles, but no difference was recognized during the subsequent ± 0.02 rad cycles. Similarly, the specimen with 0.02-rad pre-strain exhibited larger strength than the specimen with no pre-strain during the first ± 0.03 rad cycle, but no difference was recognized during the second ± 0.03 rad cycle. All three specimens exhibited very similar behavior during the final ± 0.04 rad cycles. Consequently, intermediate curing had minimal effect on the plastic deformation capacity of the beam.

Fig. 5 compares the first half cycle obtained after 0.01 or 0.02-rad pre-strain and curing. The corresponding half cycle for no pre-strain is taken from the ± 0.0075 rad cycle. Evident in this figure is the appearance of yield plateau, as the result of strain aging, and the difference in strength at the plateau depending on the extent of pre-strain. The plastic moment based on the yield strength after 0, 2, 4 or 8% pre-strain is shown for reference. For both cases of cyclic pre-strain, the strength at the plateau was close to M_p after 4% pre-strain.

Fig. 6 shows photographs of the specimens taken during the intermediate curing stage. The specimens were brought to zero chord rotation after the pre-strain cycles. Under this condition, residual deformation was hardly recognizable to the human eye. Apart from flaking of mill scale, no evidence of plastic loading history could be recognized by visual inspection. Based on 3D digital reconstruction [11], out of straightness of the flange and web, after 0.02-rad pre-strain, was 2.8 and 1.6 mm. The variation in cross-sectional dimensions was within the JIS tolerance in terms of flange squareness (0.8° opposed to limit of 1.2°) but slightly beyond the tolerance for web warping (3.6 mm opposed to limit of 2.5 mm). Therefore, the specimen after 0.02-rad pre-strain was at the borderline of passing the geometrical tolerances for newly produced steel.

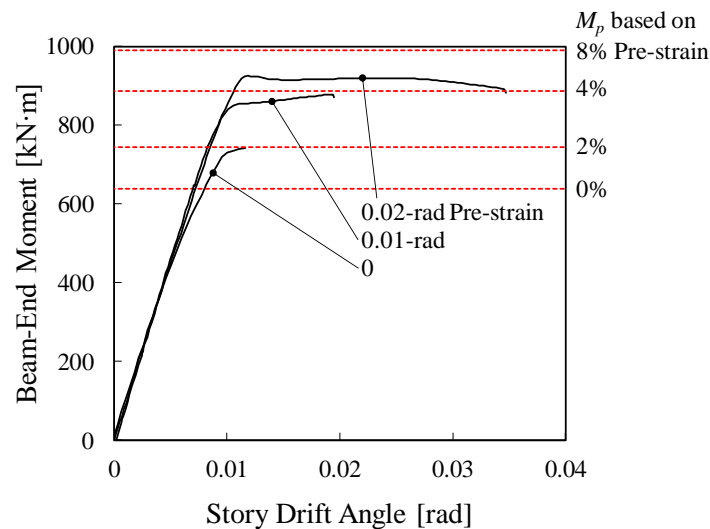


Fig. 5 – First half-cycle loading after strain aging.

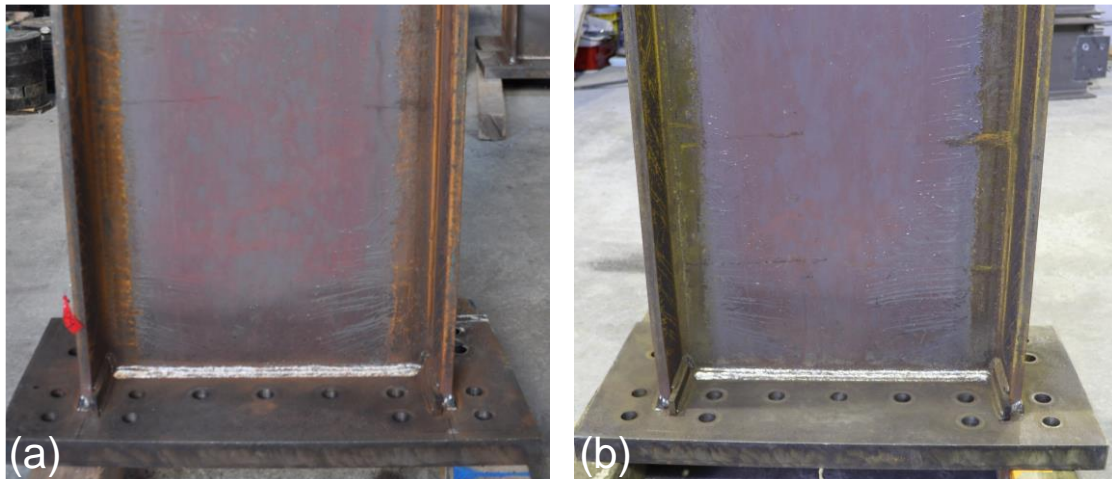


Fig. 6 – Photo of specimen during curing: (a) after 0.01-rad pre-strain; (b) after 0.02-rad pre-strain.

5. Summary

An experimental program is underway to examine the effect of plastic deformation and strain aging on the residual seismic performance of structural steel components. Coupons sampled from SS400, SN400B and SN490B steel were subjected to monotonic tension in two phases, the second phase being conducted after 1 or 3-month curing at ambient temperature. Beams constructed from the same SS400 steel were subjected to cyclic loading in two phases, the second phase being conducted after 3-month curing at ambient temperature.

In both experiments, the extent of pre-strain, or plastic deformation prior to curing, was varied between different specimens. Some of the key findings are listed below.

- Among the three steel samples, SS400 with free nitrogen content of 0.006% saw the most profound change in tension properties, while SN400B and SN490B with free nitrogen content of 0.003 and 0.002%, respectively, saw very little change.
- During the first half cycle after 0.01 or 0.02-rad pre-strain and curing, SS400 beams exhibited a yield plateau that was not seen in the specimen with no pre-strain. The significantly higher plateau strength diminished within one or two positive-and-negative loading cycles.
- The strain aging produced by 0.01 or 0.02-rad pre-strain did not affect the cyclic loading response at ± 0.04 rad. In other words, the plastic deformation capacity of the beam was not affected by strain aging resulting from cyclic pre-strain at ± 0.02 -rad.
- The residual deformation after 0.01 or 0.02-rad pre-strain was not recognizable to the human eye and was on the borderline of passing the geometrical requirements for newly produce steel.

Cyclic tension-and-compression coupon tests and cyclic-loading beam tests will be continued for the same three samples of steel. The goal of this program is to establish the correlation between steel grade, free nitrogen content, plastic loading history, etc. on the residual performance or structural steel. Such information shall contribute to promoting reuse of structural components in steel building construction.

6. References

- [1] Momtahan A, Dhakal RP, Rieder A (2009): Effects of strain-aging on new zealand reinforcing steel bars. *Bulletin of The New Zealand Society for Earthquake Engineering*, **42** (3), 179-186.
- [2] Baird JD (1971): The effects of strain aging due to interstitial solutes on mechanical properties of metals. *Metallurgical Reviews*, **5**, 1-18.
- [3] Cottrell AH, Bilby BA (1949): Dislocation theory of yielding and strain ageing of iron. *Proceeding of the Physical Society, Section A*, **62** (1-349 A), 49-61.
- [4] Pense A (2004): HPS corrugated web girder fabrication innovations, Final report, Part 4: Literature and experimental study of strain aging in HPS and other bridge steels. *Center for Advanced Technology for Large Structural Systems*, Bethlehem, USA, 7.
- [5] Wilson DV, Russell B (1960): The contribution of atmosphere locking to the strain-aging of low carbon steels. *Acta Metallurgica*, **8** (1), 36-45.
- [6] Succop LN, Pense AW, Stout RD (1970): The effect of warm overstressing in pressure vessel steel properties. *Welding Journal Research Supplement*, **49** (8), 254s-364s.
- [7] Kaufmann EJ, Metrovich B, Pense AW (2001): Characterization of cyclic inelastic behavior on properties of A572 Gr. 50 and A36 rolled sections. *ATLSS Report No. 01-13*, Bethlehem, USA.
- [8] Mojtaba MA (2015): Static strain aging in low carbon ferrite-pearlite steel: Forward and reverse loading. *Electronic Theses and Dissertations (ETDs)*, University of British Columbia, Canada.
- [9] Ono T, Murayama K, Masuda K, Sato A, Yokokawa T (2000): The experimental study on the effect of trace elements on toughness of steel plate for building structure. *Journal of Structural and Construction Engineering*, Architectural Institute of Japan, 536, 157-162. (in Japanese).
- [10] Yamada S, Takeuchi A, Kishiki S, Watanabe A (2006): Hysteresis behavior of steel affected by strain aging. *Summary of Technical Papers of Year 2006 Annual Meeting*, Architectural Institute of Japan, 927-930. (in Japanese).
- [11] Agisoft LLC (2018): *Agisoft PhotoScan User Manual*: professional edition, Version 1.4.